N63-13867
code-1

NACA

RESEARCH MEMORANDUM

FREE-FLIGHT TESTS OF 45° SWEPT WINGS OF ASPECT

RATIO 3.15 AND TAPER RATIO 0.54 TO MEASURE WING DAMPING

OF THE FIRST BENDING MODE AND TO INVESTIGATE THE

POSSIBILITY OF FLUTTER AT TRANSONIC SPEEDS

By Burke R. O'Kelly, Reginald R. Lundstrom,
and William T. Lauten, Jr.

Langley Aeronautical Laboratory
Langley Field, Va.

NATIONAL ADVISORY COMMITTEE
FOR AERONAUTICS
WASHINGTON
October 12, 1954

UNCLASSIFIED

NATIONAL ADVISORY COMMITTEE FOR AERONAUTICS

RESEARCH MEMORANDUM

FREE-FLIGHT TESTS OF 45° SWEPT WINGS OF ASPECT

RATIO 3.15 AND TAPER RATIO 0.54 TO MEASURE WING DAMPING

OF THE FIRST BENDING MODE AND TO INVESTIGATE THE

POSSIBILITY OF FLUTTER AT TRANSONIC SPEEDS

By Burke R. O'Kelly, Reginald R. Lundstrom,
and William T. Lauten, Jr.

SUMMARY

Free-flight tests have been made on two pairs of wings of aspect
ratio 3.15, taper ratio 0.54, and 45° sweepback in the transonic speed
range to measure wing damping and to investigate the possibility of flutter.
The first bending and torsional frequencies for the first model were 37
and 148 cycles per second and the corresponding values for the second
model were 31 and 122 cycles per second. The mass ratio of the wings was
similar to that of current fighter-type wings at about 30,000 feet.
Flutter did not occur during either flight. The maximum Mach number of
the first model was 1.50 and for the second model the maximum Mach num-
ber was 1.39. One pair of wings was equipped with small devices to excite
the bending mode of the wings and the total damping was measured from the
resulting oscillations.

The wing-exciting technique as utilized is useful in flutter work
especially in that information can be obtained on flutter susceptibility
even though flutter does not occur.

INTRODUCTION

Free-flight tests at zero lift at transonic speeds have been con-
ducted by the Langley Laboratory to determine the wing-damping character-
istics and to investigate the possibility of flutter of these wings.

In order to study the tendency to flutter of this low-aspect-ratio swept wing, devices were installed in the wings of one of the models to excite a free vibration of the wing primarily in the first bending mode in order to measure the total damping present at various times during the flight. The technique provides a means for determining the margin of safety if flutter does not occur. The experimental damping values are compared with damping values obtained from theory and provide a more comprehensive basis for correlation than merely comparing calculated and experimental flutter speeds.

The method of determining damping at various airspeeds by vibrating a wing and measuring the rate of decay of the vibration has been used previously in wind tunnels. (For example, see ref. 1.) The problems encountered in applying this technique to rocket-powered free-flight models are development of a device which will initiate the vibration and obtaining a proper measure of the wing damping.

SYMBOLS

A_p aspect ratio of one exposed wing panel, $\dfrac{l^2}{\text{Area of one exposed panel}}$

a nondimensional location of elastic axis of wing section measured from midchord, positive rearward, $\dfrac{x_{ea}}{b} - 1$

$a + x_\alpha$ nondimensional location of center of gravity of wing section measured from midchord, positive rearward, $\dfrac{x_{cg}}{b} - 1$

b semichord of test wing normal to quarter-chord line, ft

c local wing chord measured in free-stream direction, in.

δ logarithmic decrement, $\dfrac{1}{n} \log_e \dfrac{\text{Amplitude at 0 cycles}}{\text{Amplitude at n cycles}}$

EI bending stiffness, lb-in.^{2}

f frequency, cps

g total damping coefficient, δ/π

GJ torsional stiffness, lb-in.^{2}

I_α polar mass moment of inertia about elastic axis per unit length, ft-lb-sec^2/ft

I_p polar mass moment of inertia about center of gravity per unit length, ft-lb-sec^2/ft

l exposed semispan of wing normal to model center line, in.

Λ sweepback at quarter-chord line, deg

λ taper ratio of exposed wing panel, c_t/c_r

M Mach number

m mass of wing per unit length, slugs/ft

μ mass ratio, $m/\pi\rho b^2$

ρ atmospheric density, slugs/cu ft

r_α^2 square of nondimensional radius of gyration about elastic axis, I_α/mb^2

S wing area including body intercept, sq ft

t flight time from launching, sec

t/c airfoil thickness ratio

V velocity, fps

x_{cg} distance of center of gravity of wing section behind leading edge normal to quarter-chord line, ft

x_{ea} distance of elastic axis of wing section behind leading edge normal to quarter-chord line, ft

Subscripts:

r root

t tip

h_1 first bending

h_2 second bending

α_1 first torsion (uncoupled) about elastic axis

APPARATUS AND METHODS

Models

The models used in these tests (except for the test wings) were of the same type as those described in reference 2; the launching technique was also the same. The booster rockets used were such that the range of low acceleration of the models alone would be from approximately $M = 0.9$ to $M = 1.5$. A sketch of the general model configuration is shown in figure 1, and a photograph of a model is shown as figure 2.

Wings

The exposed wing panels, which were made of laminated spruce, were swept back 45° at the 25-percent-chord line and had modified NACA 0009 airfoil sections at the roots and modified NACA 0007 airfoil sections at the tips. Each exposed wing panel had a taper ratio of 0.54, and the aspect ratio of the wings including the area projected into the fuselage was 3.15. The bending frequency was about 34 cycles per second and the torsional frequency was about 135, averaged for the four test wings. The mass ratio μ at sea level was similar to that of current fighter-type wings at about 30,000 feet.

Table I lists the structural properties of the two pairs of model wings. The frequencies listed were measured for each wing mounted independently and were checked after mounting the wings in the test vehicle. Stiffness and mass and inertia distributions along the quarter-chord line are presented in figures 3 and 4.

The torsional stiffness GJ was determined experimentally by applying known moments to the wing tip and measuring the twist at various span-wise stations. The bending stiffness EI was measured by applying loads to the wing tip and measuring the slope of the deflection curve at various spanwise stations. The differences in EI and GJ for the four test wing panels were negligible. The mass and inertia parameters were calculated from measured wing densities. Variation of the elastic-axis position along the span as determined with the wings installed in the model is presented in table II. Since a swept wing has no elastic axis in the commonly accepted sense, the values given are the chordwise locations where a point load may be applied normal to the plane of the wing without causing rotation of the loaded station in a plane normal to the quarter-chord line.

Wing Exciters

The second of the two models had a device called an exciter installed at the point of maximum thickness near the tip of each wing (fig. 1) to cause the wings to vibrate primarily in free bending since calculations had indicated this to be the critical mode. Photographs of the installation may be seen in figure 5, and a sectional drawing showing the different parts is presented in figure 6.

Each barrel-chamber block, which was made of steel, contained three barrels of 0.309-inch diameter. A lead slug was forced into each barrel to a depth of 0.25 inch and filed off smooth. A piece of hard brass shim stock 0.0015 inch thick was held over the ends of the slugs by an aluminum-alloy mounting plate. This shim stock served as a rupture disk and prevented the slug from leaving the barrel until the chamber pressure reached about 700 lb/sq in. The total impulse was on the order of 0.1 pound-second and the time for the slug to leave the barrel was about 0.002 second.

Each igniter holder contained a small electric igniter and about 0.5 gram of fast-burning fine black powder and was covered with a disk of cellophane tape to keep the powder from spilling out.

The igniter leads were connected to a firing unit which was a rotary switch driven by a small electric motor. This motor was energized by a switch which closed at booster separation. The firing unit was preset and wired in such a way that the six exciter units began to fire in alternate wings about 1 second after booster separation and at half-second intervals thereafter. In this way, most of the low-acceleration test range between booster separation and maximum velocity was utilized.

The weight of each barrel-chamber block with igniter holders was 0.25 pound , not including the lead slugs which weighed about 0.011 pound each. The wood cut out of each wing for installation of the exciter unit weighed about 0.04 pound.

Instrumentation

An eight-channel telemeter was installed in each model which transmitted continuous readings from bending and torsion strain gages on each wing, angle-of-attack indicator, total-pressure pick-up, and normal and longitudinal accelerometers located near the model center of gravity. The strain gages were located on the wing so that the bending gages were practically insensitive to torsional strain, but the torsion gages could not be made insensitive to bending strain. A spinsonde receiver, picking up the signal from the telemeter antenna on the model, furnished rate-of-roll information whereas the velocity of the model was obtained from

information given by a CW Doppler radar set. The position of the models in space was determined from data obtained from a pulse-type tracking radar. Atmospheric conditions prevailing at the times of the flights of the models were recorded by radiosonde. The models were launched at the Langley Pilotless Aircraft Research Station at Wallops Island, Va.

RESULTS AND DISCUSSION

Flight-Test Results

Model 1 reached a maximum Mach number of 1.50 at near-zero lift with no vibrations being visible on the wing strain-gage traces. A time history of the flight showing velocity, Mach number, and air density may be seen in figure 7(a).

Model 2 reached a maximum Mach number of 1.39 at near-zero lift and also had no vibrations on the wing strain-gage traces except those caused by the exciters deflecting the wings. A time history of the flight showing velocity, Mach number, and air density is shown as figure 7(b). The exciters and the timing unit performed satisfactorily and initiated wing vibrations at Mach numbers of 0.93, 1.01, 1.09, 1.16, 1.21, and 1.29.

Analysis and Discussion

A portion of the telemeter record of the second model, showing typical wing oscillations when one of the exciter units fired, is presented in figure 8. As may be seen in figure 8, not only does the disturbed wing vibrate but some of the energy is absorbed by the opposite wing so that it also vibrates. The rate of decay of the oscillations in the excited wing depends not only upon the damping present but also upon the rate at which energy is absorbed by the opposite wing. The wing at the peak of its deflection (bending) following exciter firing possessed a certain amount of potential energy equal to $Ky^2/2$ where K is the spring constant (pounds per inch deflection at a certain point on the wing) and y is the actual deflection of the given point. During the vibrations which followed, the energy was transformed back and forth between kinetic and potential energy. If an envelope curve is drawn through the vibration peaks, the total energy at a given time is $Ky_1^2/2$ where y_1 is the distance out to the envelope curve at that time and the difference between the energy at two such times is the energy lost in damping. If, however, as in this case, some of the energy was used to vibrate the opposite wing (which also possessed damping) this energy must also be accounted for. By fairing an envelope curve through the peaks of the opposite wing motions, its change in energy over a given period of time may also be determined.

Since the two wings had practically identical properties such as spring constant, natural frequency, structural damping, and so forth, and presumably the same load distribution, the excited wing should have had the same aerodynamic damping characteristics as the opposite wing. Therefore, the difference between the sum of the energies of the two wings at one time and the sum of the energies at another time is the energy lost in total damping over that time. The data were reduced by first adjusting the left wing trace of figure 8 so that it had the same number of inches displacement on the record per inch wing deflection as did the right wing. The trim lines were then determined and envelope curves faired in. Composite envelope curves were then constructed by taking the square root of the sum of the squares of distances from the individual wing envelope curves to the trim line. The logarithmic decrement of this resultant oscillation was found in the usual manner and the total damping coefficient g was then computed from the relation

$$g = \frac{\delta}{\pi}$$

where δ is the logarithmic decrement of the decaying oscillation. Values of the damping coefficient were found for each of the six separate pulses and are plotted as a function of Mach number in figure 9. This coefficient is a total damping coefficient including both aerodynamic and structural damping of the wings. The scatter of the points is believed to be a result of poor adjustment made so that the left-wing trace would have the same sensitivity on the record as the right-wing trace. The strain gages had obviously changed from the original calibration. The adjustment factor used was the factor necessary to give equal displacements on the record for the bending gages on each wing when the model was disturbed after booster separation. This condition, of course, assumes that the wing loading is symmetrical over this calibration period, which is not necessarily true. It might be mentioned that, if this adjustment factor were about 30 percent lower, the damping points would fall on a smooth curve. Shown also in figure 9 is a plot of the frequency of the wing oscillation in flight as a function of Mach number.

In order that a comparison might be made between the results of the present test and other experimental data and theory, the damping curve of figure 9 is replotted in figure 10 with the Mach number range extending back to zero in order to show values of structural damping. The value of structural damping for the wings of the present test was obtained from vibration tests in still air on the ground. During these ground tests as in the flight tests, when one wing was disturbed, the opposite wing also vibrated. In the case of the ground tests, the model support may also have vibrated and contributed to the damping. Past experience with wooden wings, however, indicates that the determined value shown is of the proper order of magnitude.

The other curve in figure 10 is a theoretical curve obtained from the results of calculations of damping made on the flight-tested wings for model 2 by using the simplified flutter theory of reference 3. These calculations were determined from a strip analysis based on a two-dimensional unsteady compressible-flow theory and utilize a method of flutter analysis which includes the effects of sweep and mode shape but not of finite span. The modes used were wing first bending and wing first torsion. The model instrumentation showed that the body motions were extremely small and it is felt that they had negligible effects on the results. Calculations were made by using aerodynamic coefficients for normal-flow Mach numbers of 0, 0.5, and 0.7. The damping was determined for the branch of the flutter solution which gave the lowest value of flutter speed. In order to determine that there was no sudden change in the mode of oscillation, the value of the frequency was also obtained from the calculations. This frequency varied from a minimum value of 33 cycles per second to a maximum value of 57 cycles per second for the data calculated for the three Mach numbers. These values compare favorably with those obtained in the flight test. The theoretical curve in figure 10 is a composite curve of the results obtained from the three cases calculated. In figure 10, the normal-flow Mach numbers have been converted to free-stream values for plotting purposes.

It should be noted that there are differences between the physical aspects of the wing and the simplifying assumptions of the theory. Probably, the primary difference is in the two-dimensional flow of the theory (each strip of wing acted on by two-dimensional flow) and the three-dimensional flow to which the wing is actually subjected. Furthermore, the theory assumes a wake which is harmonically distributed over an infinite distance behind the wing whereas for this experiment the wing starts its second cycle of oscillation (at $M = 1.0$) when the wake from the beginning of the first oscillation is approximately 50 chord lengths behind the wing. A third difference is that the damping calculated from the theory is that value (with opposite sign) which would allow an oscillation to be sustained at a constant amplitude, whereas the experimental damping values are obtained from a decrease in the amplitude of the oscillation. It is felt that these differences, particularly the finite-span effect, are sufficient to cause the theory to yield different answers for flutter speed and damping than were obtained experimentally.

Although, over a large speed range, the calculations yield a value of damping approximately double that of the experimental results, the decrease in the calculated damping values is much more marked in the transonic range. Calculated damping values above a free-stream Mach number of 1.0 are not presented because compressible coefficients for this wing were not available between free-stream Mach numbers of 1.0 and 1.41. Calculations at $M = 1.41$ yielded no solution and indicated that there was no flutter at supersonic speeds. If incompressible coefficients are used, a flutter speed corresponding to $M = 1.21$ is obtained as shown

in figure 10. This estimate of flutter speed is a conservative one since the first wings tested flew to $M = 1.5$ and the second pair flew to $M = 1.39$ without encountering flutter.

CONCLUSIONS

Two pairs of wings of $45°$ sweepback, aspect ratio 3.15, and taper ratio 0.54 with first bending frequencies about 34 cycles per second and first torsional frequencies about 135 cycles per second having a mass ratio similar to that of current fighter-type wings at 30,000 feet have been tested near zero lift in free flight by means of the rocket-powered model technique.

The total damping in the bending mode was measured on the wings of one of the models tested. Theoretical studies yield much higher damping values over a large portion of the speed range (Mach numbers of 0 to 1.1) but decrease more rapidly than the experimental values in the higher transonic range.

No flutter occurred during the flights of either model, one model reaching a Mach number of 1.50 and the other, a Mach number of 1.39. A flutter speed obtained from the theoretical studies by using incompressible coefficients proved to be conservative.

The wing-exciting technique as utilized is useful in flutter work especially in that information can be obtained on flutter susceptibility even though flutter does not occur.

Langley Aeronautical Laboratory,
    National Advisory Committee for Aeronautics,
        Langley Field, Va., March 5, 1954.

REFERENCES

1. Schwartz, Martin D., and Wrisley, Donald L.: Investigation of Flight Flutter Testing Techniques. Preprint No. 317, S.M.F. Fund Preprint, Inst. Aero. Sci., Jan.-Feb. 1951.

2. Lauten, W. T., Jr., and O'Kelly, Burke R.: Results of Two Experiments on Flutter of High-Aspect-Ratio Swept Wings in the Transonic Speed Range. NACA RM L52D24b, 1952.

3. Barmby, J. G., Cunningham, H. J., and Garrick, I. E.: Study of Effects of Sweep on the Flutter of Cantilever Wings. NACA Rep. 1014, 1951. (Supersedes NACA TN 2121.)

UNCLASSIFIED

TABLE I

STRUCTURAL CHARACTERISTICS OF THE MODEL WINGS

	Model 1		Model 2	
	Left	Right	Left	Right
A_p	1.34	1.34	1.34	1.34
a	0.436	0.370	0.440	0.380
$a + x_\alpha$	-0.134	-0.134	-0.248	-0.234
$r_\alpha{}^2$	0.5483	0.4767	0.6900	0.5930
f_{h_1}, cps	37.0	37.0	30.5	31.5
f_{h_2}, cps	154.0	144.0	150.0	168.0
f_{α_1}, (uncoupled), cps . . .	134.7	160.5	120.5	123.0
μ_r, at maximum velocity . .	40.25	40.69	47.48	46.56
μ_t, at maximum velocity . .	32.35	32.70	38.16	37.42

TABLE II

VARIATION OF THE ELASTIC-AXIS POSITION ALONG THE SPAN

Inches along leading edge from root	$\dfrac{x_{ea}}{2b} \times 100$ for -			
	Model I		Model II	
	Left wing	Right wing	Left wing	Right wing
11.25	----	74.0	----	----
11.75	72.7	----	78.0	73.2
14.25	----	67.9	----	----
14.75	70.9	----	72.5	73.1
17.00	----	68.9	----	----
17.75	70.8	----	73.0	67.9
21.00	----	68.6	----	----
21.25	----	----	71.7	69.6
21.75	73.0	----	----	----
23.75	77.6	77.9	70.0	68.9

λ		16.36 in.
c_r		15.80 in.
c_t		8.54 in.
t_r/c_r		9 %
t_t/c_t		7 %
Λ		45°
S		3.82 sq ft
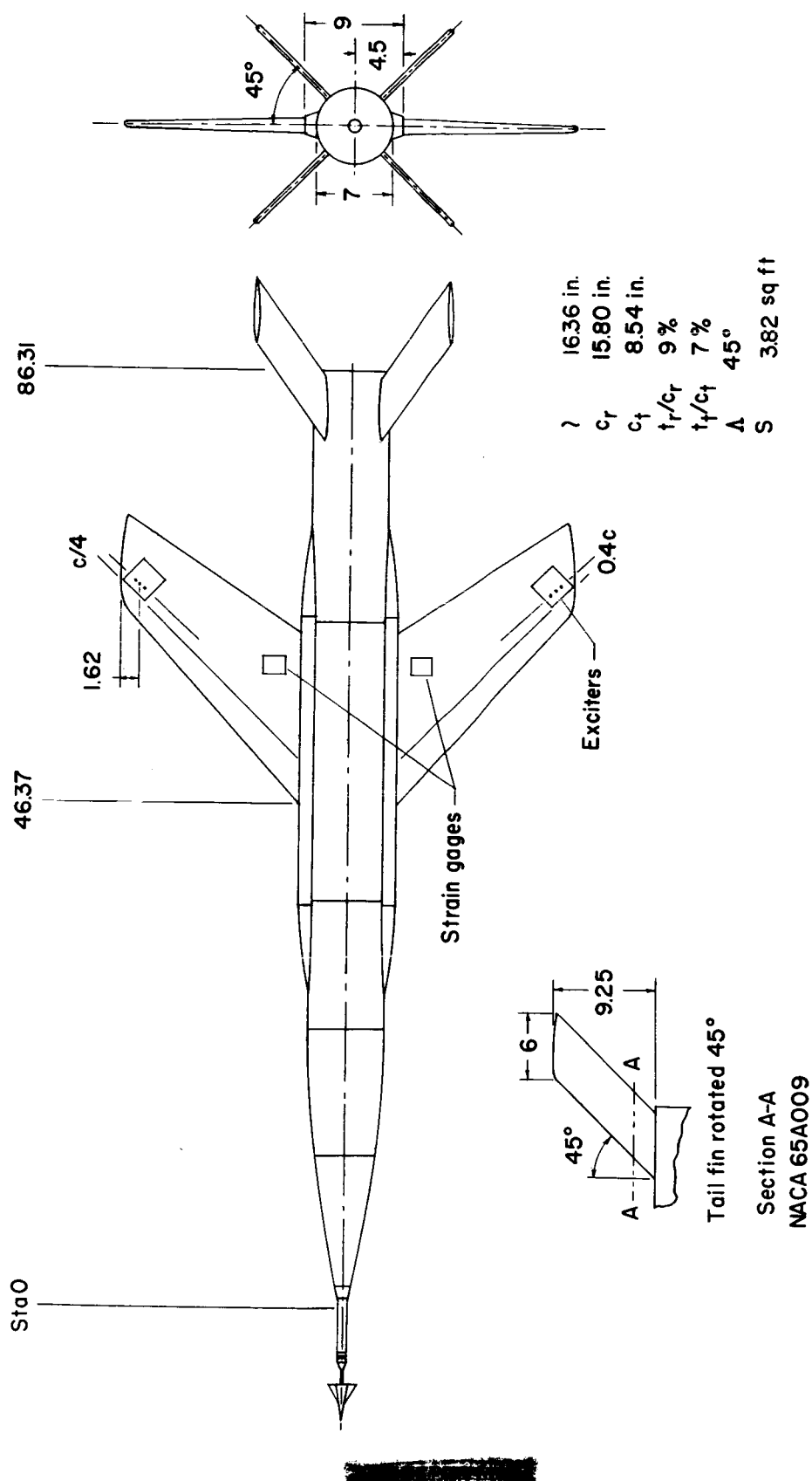
Figure 1.- General model arrangement. (All dimensions are in inches.)
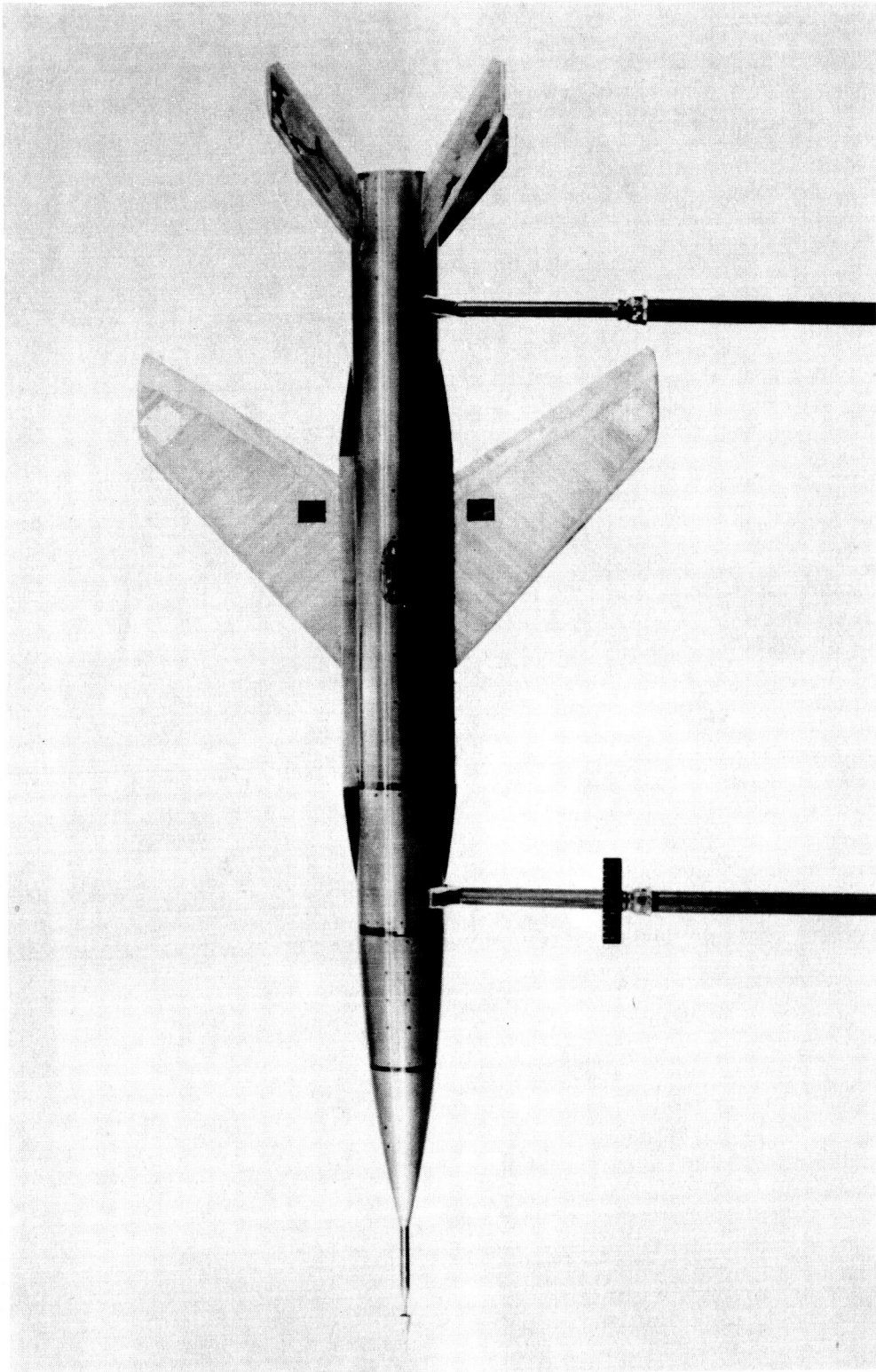
Figure 2.- Photograph of model 2.

L-78115.1

UNCLASSIFIED
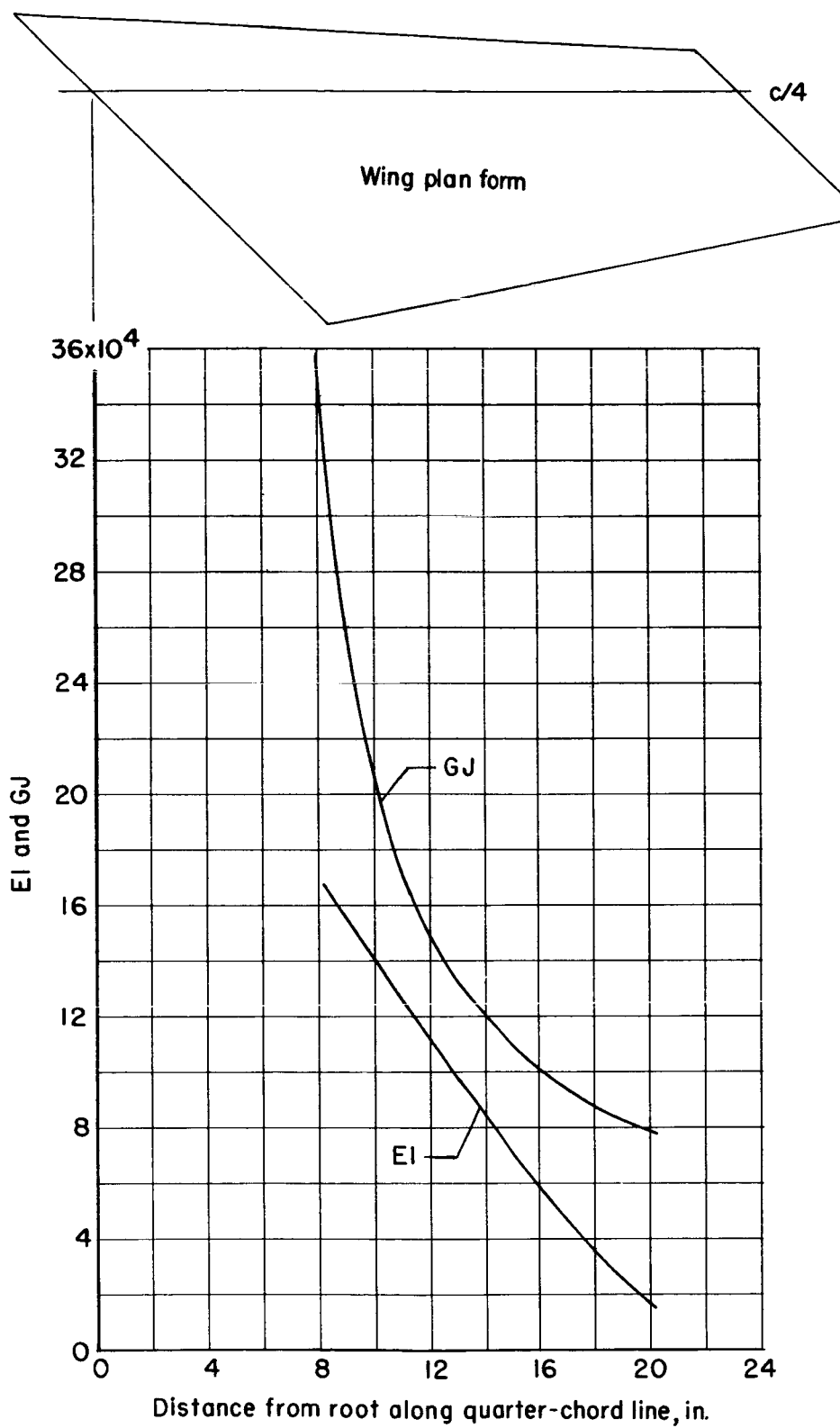
Figure 3.- Measured distribution of stiffness.
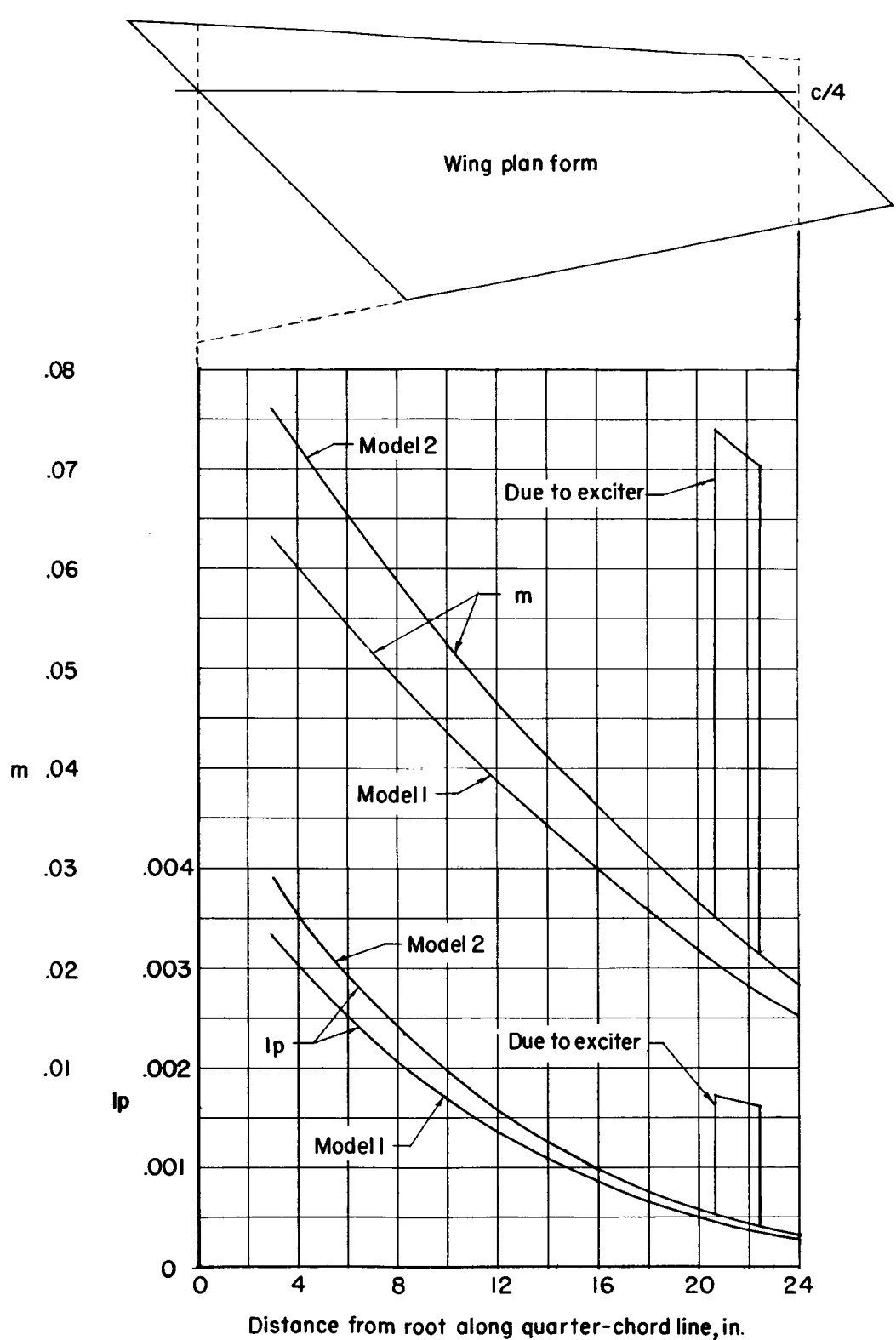
Figure 4.- Calculated distribution of mass and inertia for right wings.
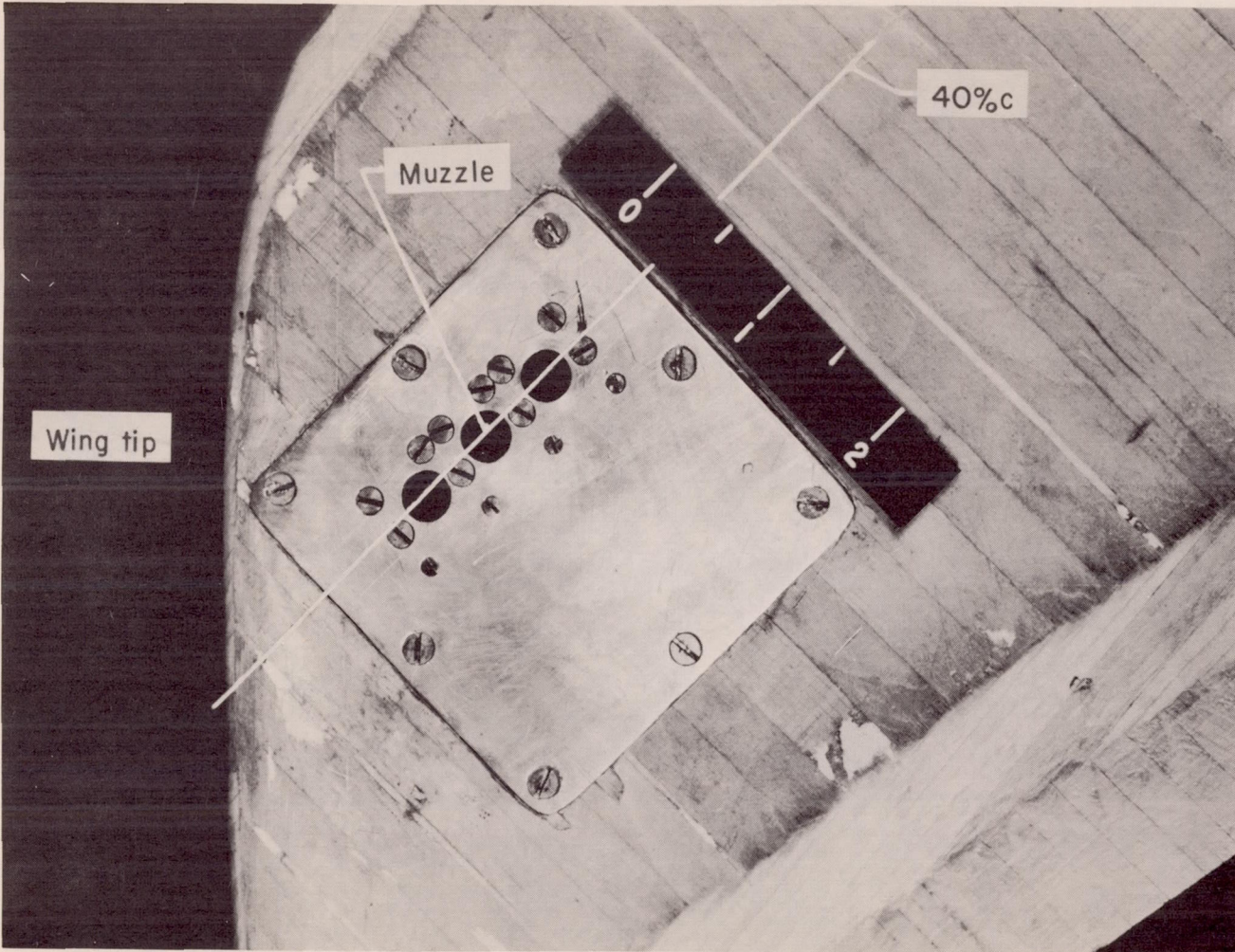
(a) Bottom view.

L-78117.1

Figure 5.- Photograph of exciter installation.
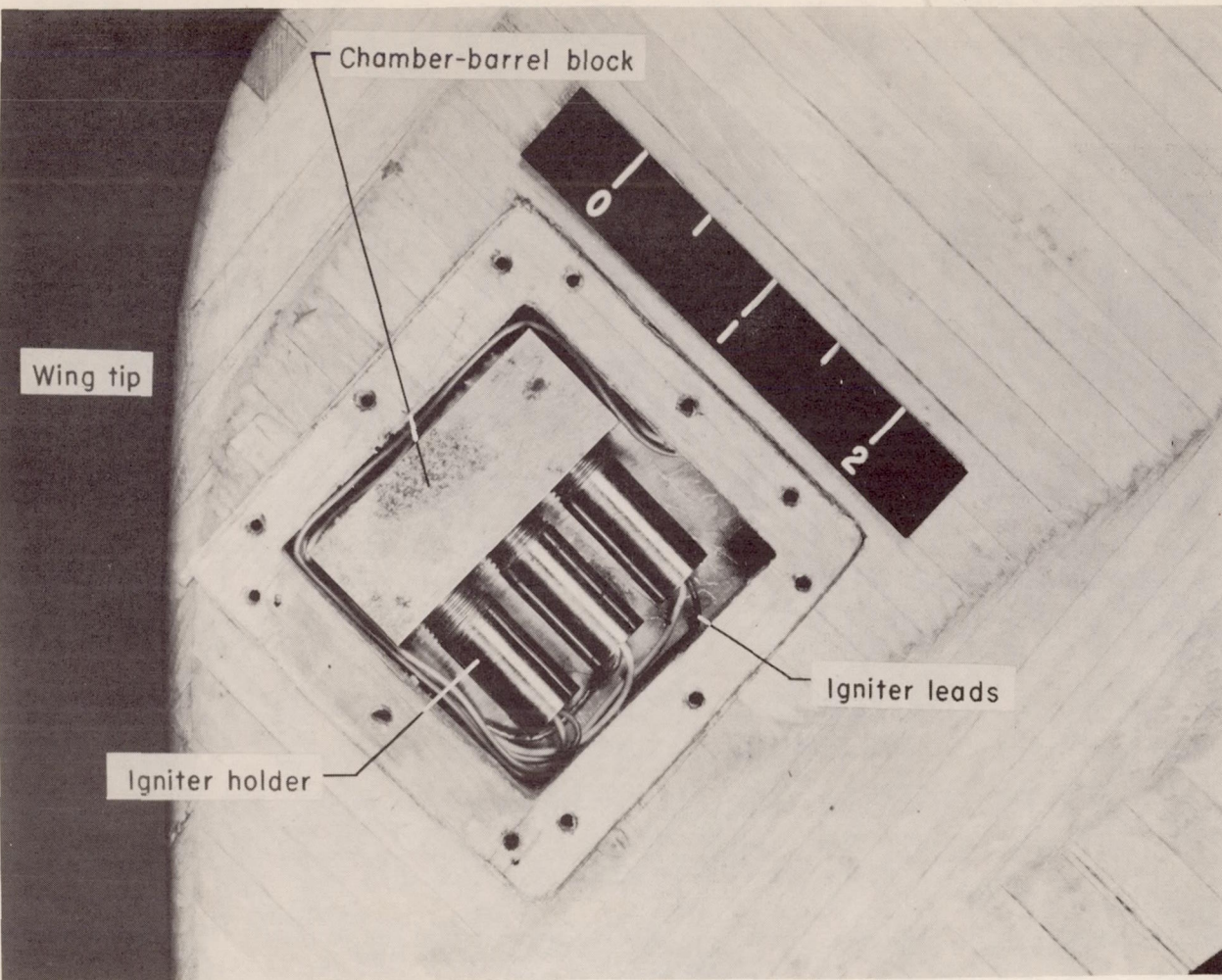
(b) Top view.

Figure 5.- Concluded.

L-78116.1
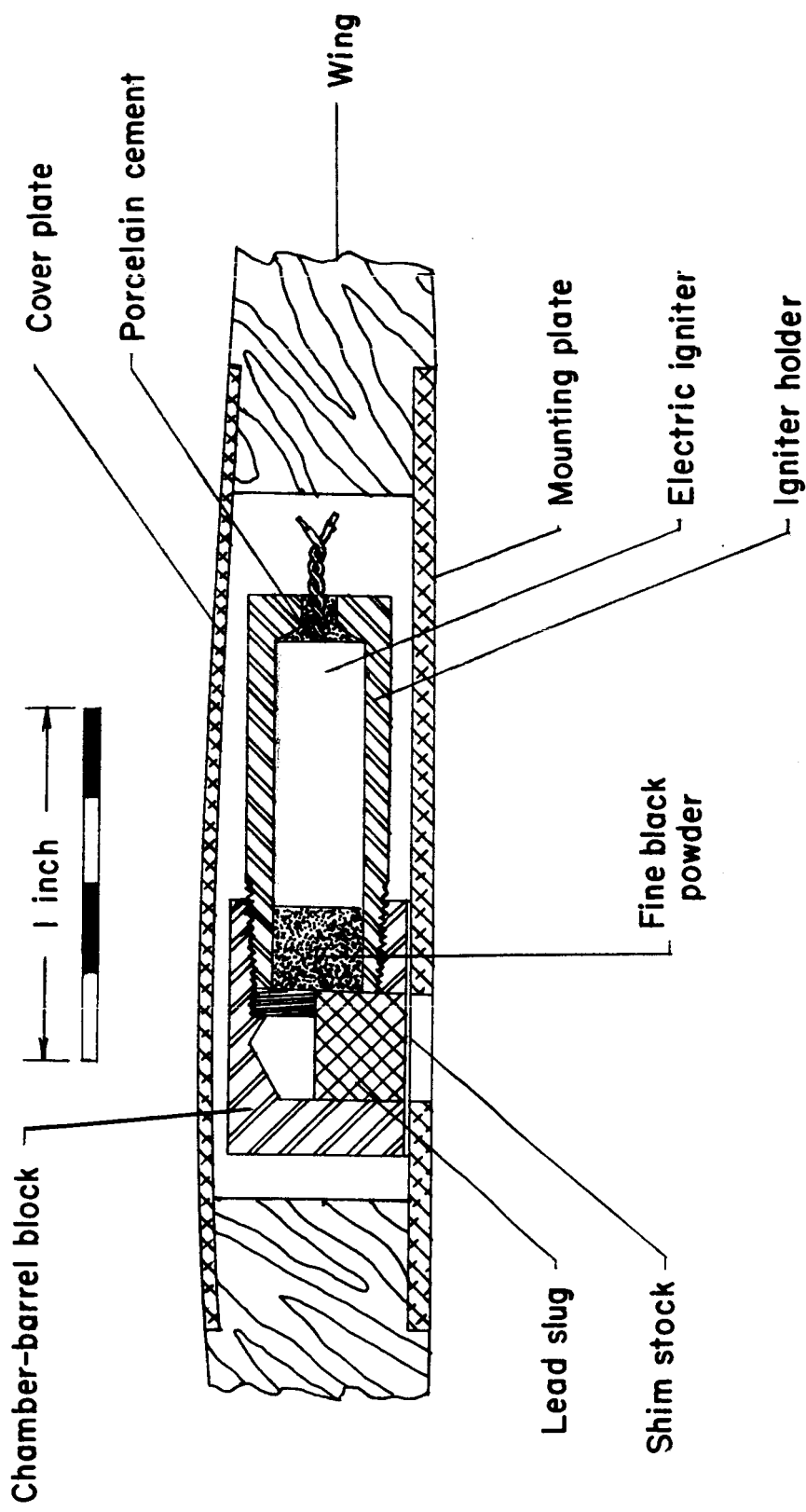
Figure 6.- Sectional view of exciter installation.
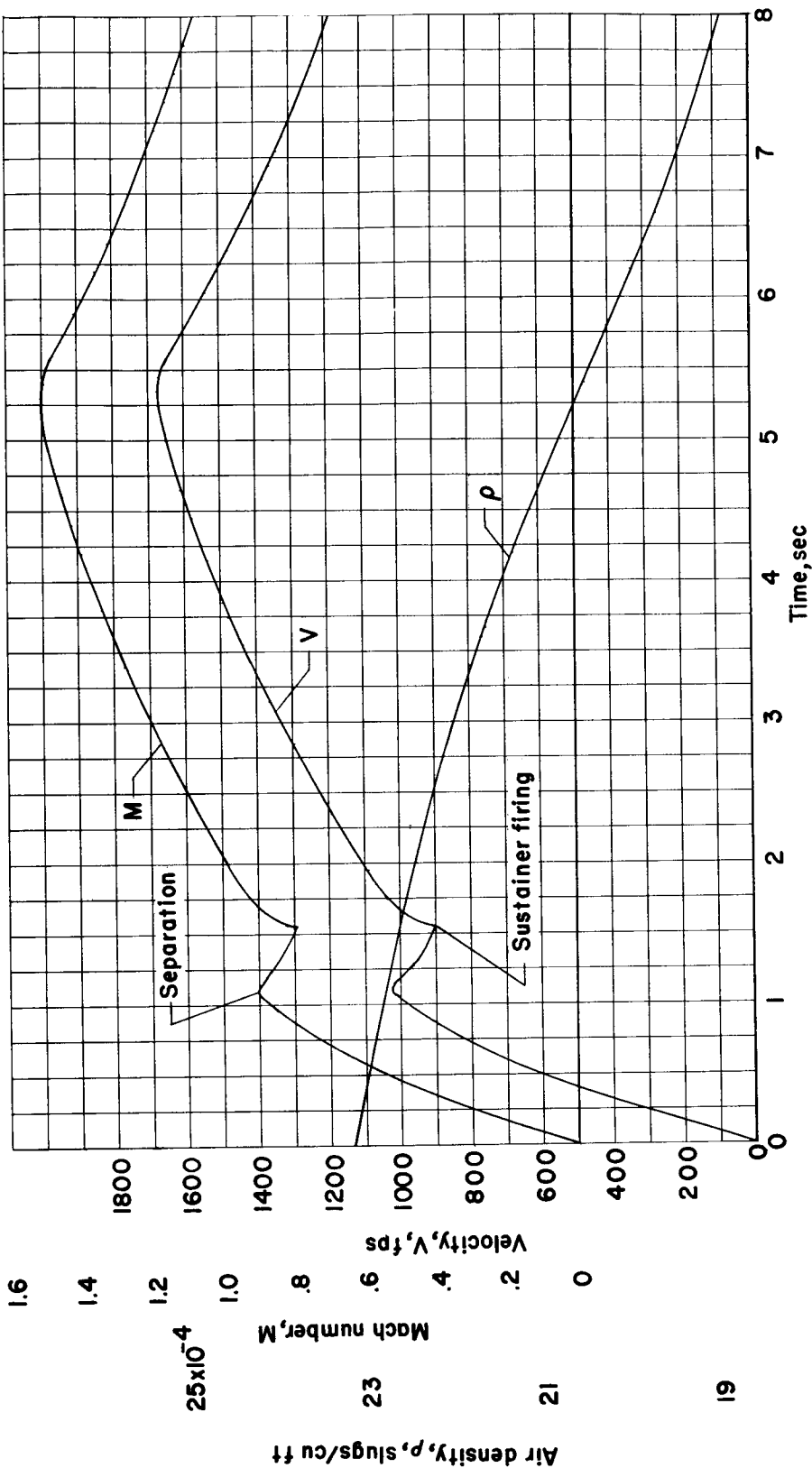
(a) Model 1.

Figure 7.- Time history showing velocity, Mach number, and air density.
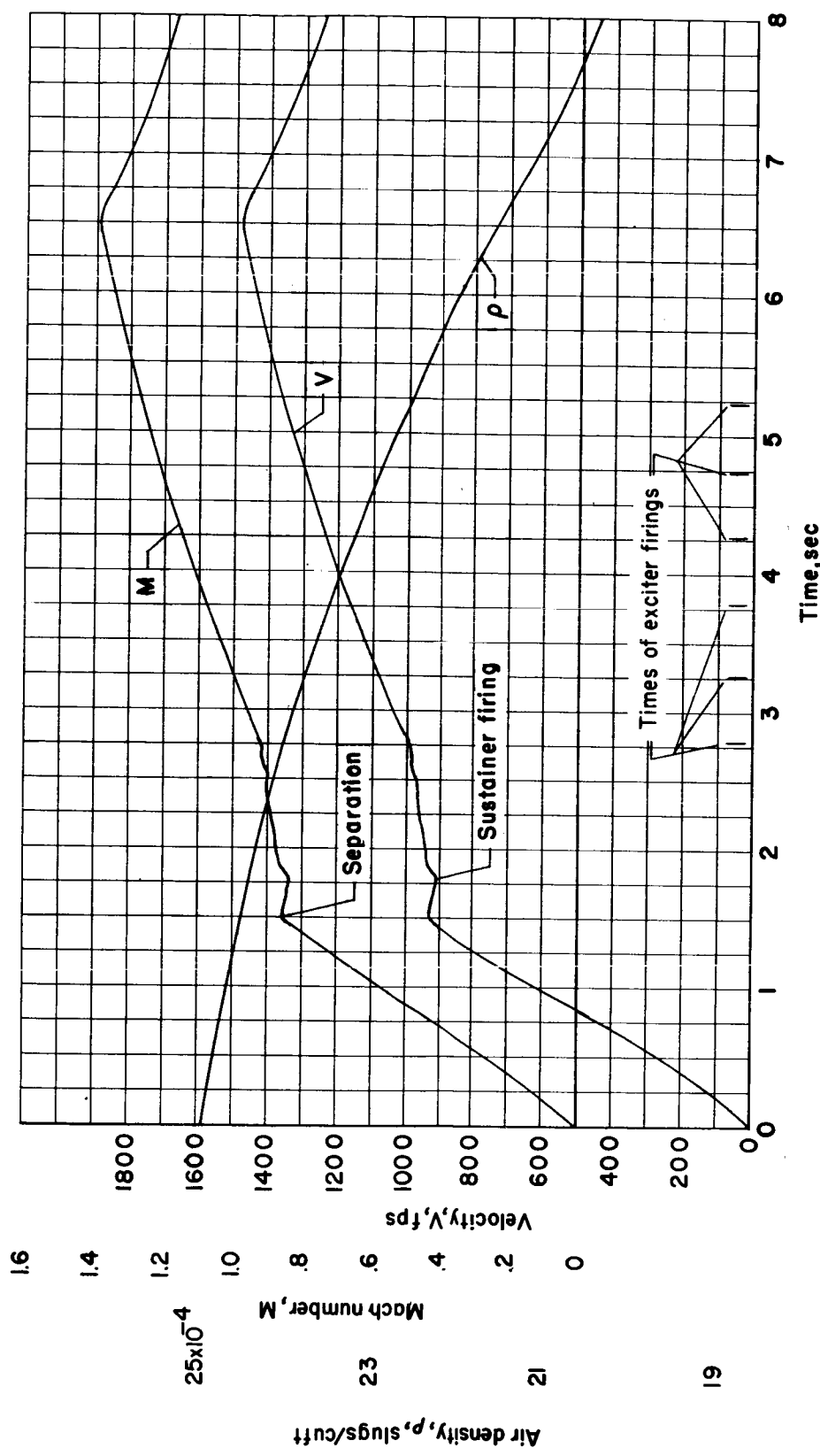
(b) Model 2.

Figure 7.- Concluded.
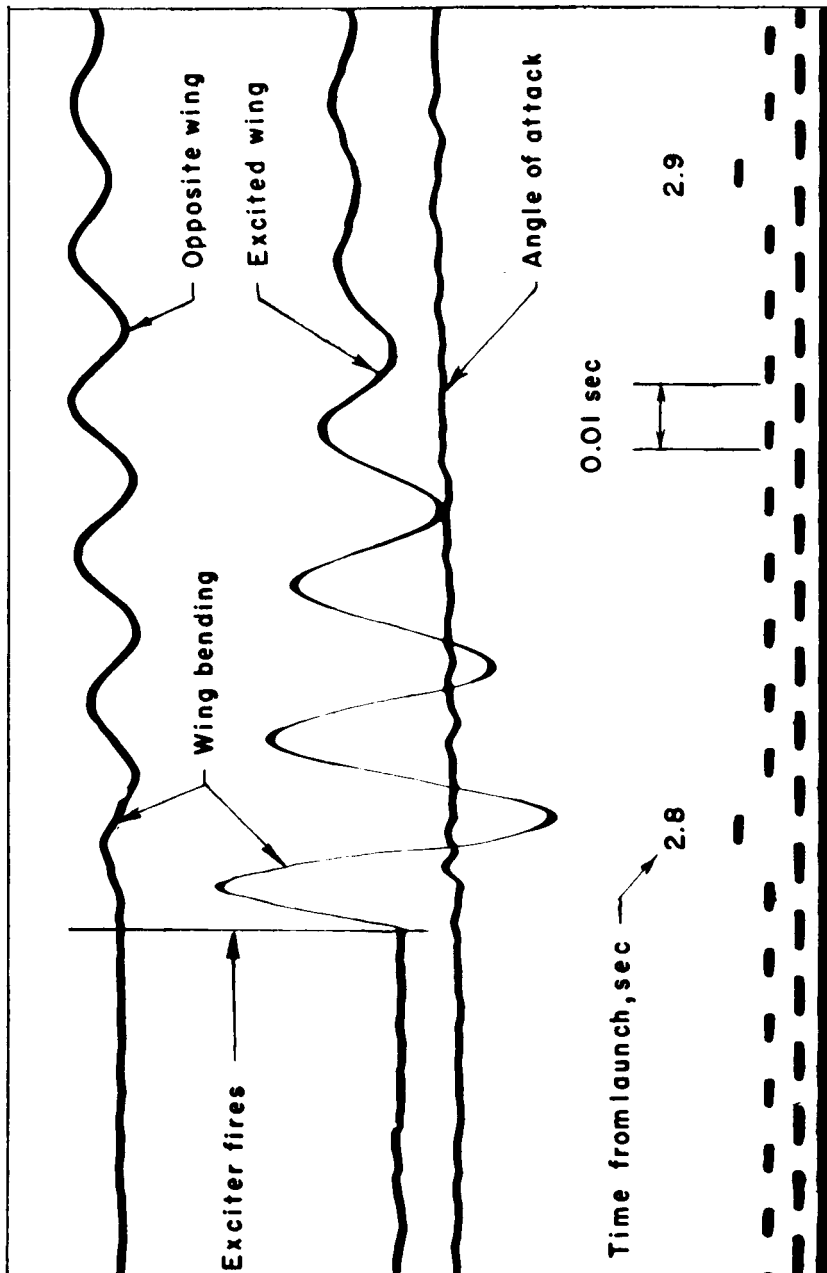
Figure 8.- Portion of telemeter record.
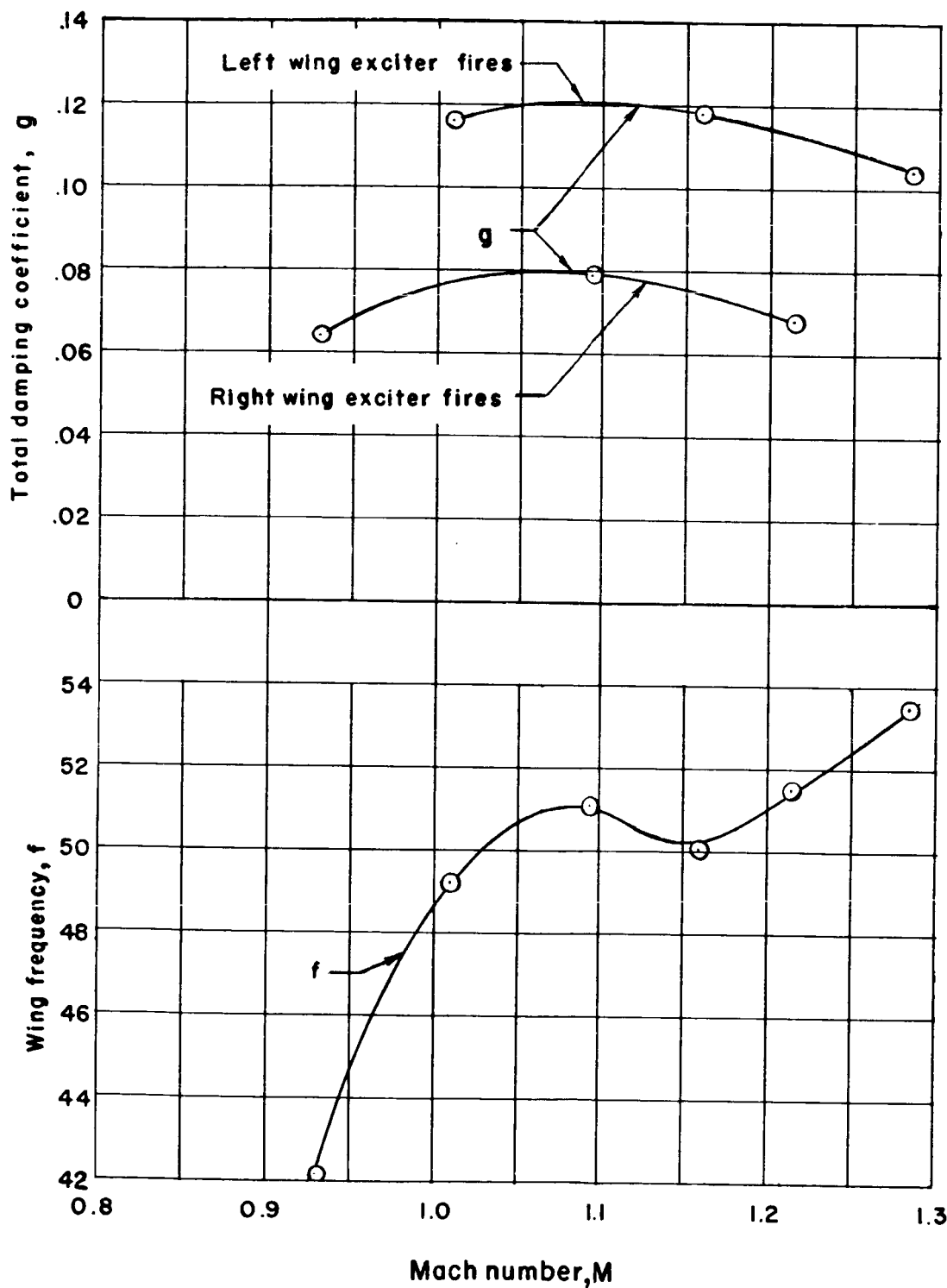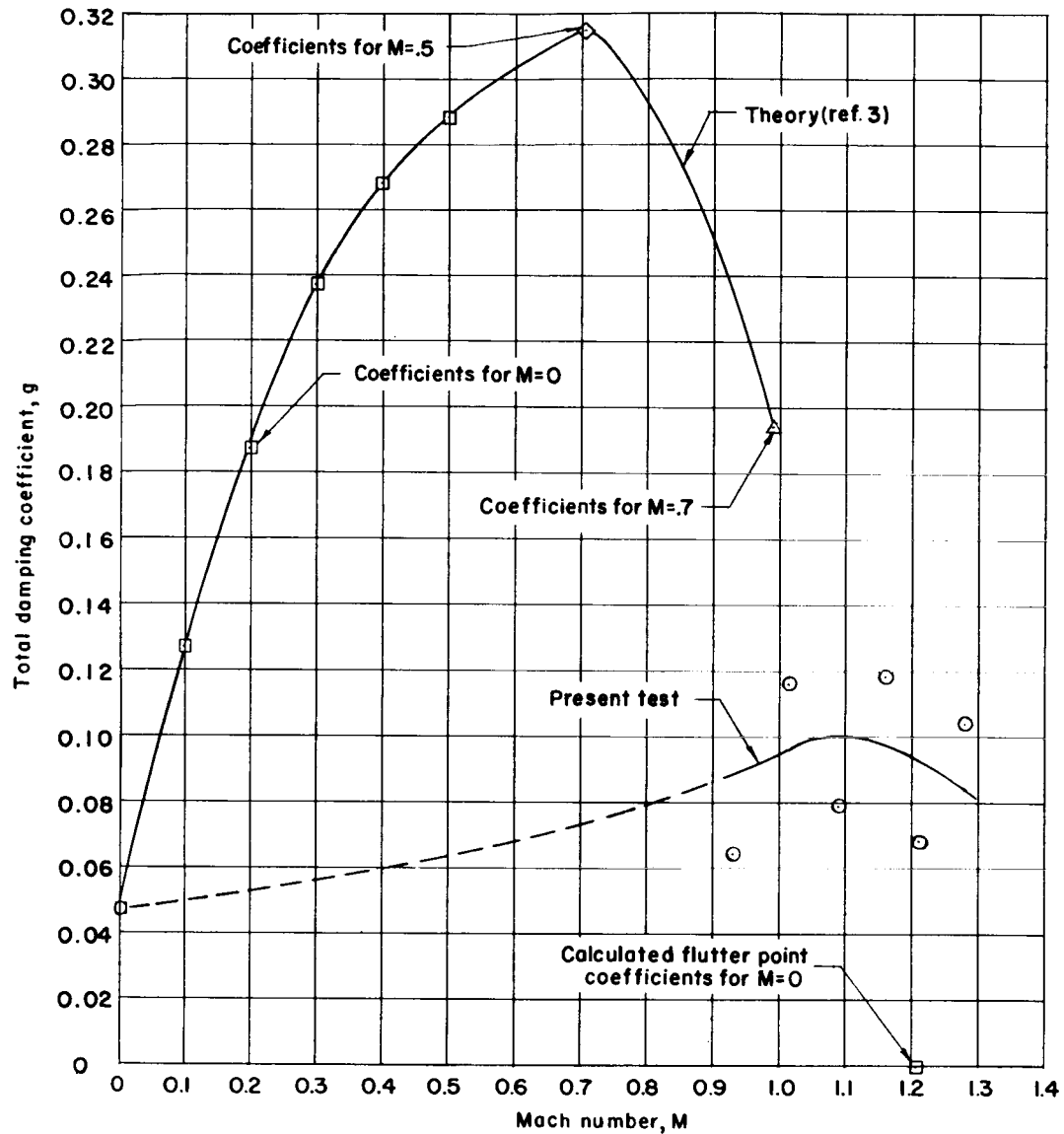
Figure 9.- Damping coefficients and wing frequency.

Figure 10.— Comparison of experiment and theory.